



U.S. DEPARTMENT OF
ENERGY

PNNL-25450

Prepared for the U.S. Department of Energy
under Contract DE-AC05-76RL01830

Decoupled Modulation Control

S Wang
Z Huang

R Huang
R Diao

May 2016



Pacific Northwest
NATIONAL LABORATORY

*Proudly Operated by **Battelle** Since 1965*

Abstract

The objective of this research work is to develop decoupled modulation control methods for damping inter-area oscillations with low frequencies, so the damping control can be more effective and easier to design with less interference among different oscillation modes in the power system.

A signal-decoupling algorithm was developed that can enable separation of multiple oscillation frequency contents and extraction of a “pure” oscillation frequency mode that are fed into Power System Stabilizers (PSSs) as the modulation input signals. As a result, instead of introducing interferences between different oscillation modes from the traditional approaches, the output of the new PSS modulation control signal mainly affects only one oscillation mode of interest.

The new decoupled modulation damping control algorithm has been successfully developed and tested on the standard IEEE 4-machine 2-area test system and a miniWECC system. The results are compared against traditional modulation controls, which demonstrates the validity and effectiveness of the newly-developed decoupled modulation damping control algorithm.

Contents

Abstract	i
Contents	1
Figures	2
1.0 Proof of concept	3
1.1 Background and milestone summary	3
1.2 Concept of decoupling oscillation modes	3
1.3 An example of a successful proof of concept.....	5
2.0 A real-time signal decoupled approach through band pass filter.....	7
2.1 Real time decoupling approach through band pass filters.....	7
2.2 Implementation of the approach.....	8
2.3 Test results in the two-area four-machine system.....	10
2.4 Test results in the mini WECC system.....	14
3.0 Conclusions	20
4.0 References	21

Figures

Figure 1.1. Two-area, four-machine system	5
Figure 1.2. Traditional modulation control	6
Figure 1.3. Decoupled modulation control	6
Figure 2.1 Band pass filter	7
Figure 2.2 Frequency characteristic with $\omega_0=1$ and various values of Q, for 0.5 to 5. [1].....	8
Figure 2.3 M file for the band pass filter	9
Figure 2.4 Two-area four-machine system	10
Figure 2.5 Tie-line power oscillation without PSS	10
Figure 2.6 Frequency spectrum of the tie-line power oscillation in Fig. 5	11
Figure 2.7 Tie-line power oscillation with band-pass filter of 1.15 Hz	12
Figure 2.8 Frequency spectrum of the tie-line power oscillation in Fig. 7	12
Figure 2.9 Tie line power oscillation with four PSS	13
Figure 2.10 Frequency spectrum of the power line power oscillation in Fig. 7.....	13
Figure 2.11 Performance comparison	14
Figure 2.12 Simplified WECC System One-Line Diagram.....	15
Figure 2.13 Mode shape for 0.324-Hz Alberta mode in mini WECC system	16
Figure 2.14 Mode shape for 0.626-Hz BC mode in mini WECC system	17
Figure 2.15 Tie-line flow (one line) from Las Vegas (Bus 57) to Los Angeles (Bus 113).....	18
Figure 2.16 Frequency spectrum of the tie-line flow (Bus 57 to Bus 117) for the case without decoupled damping control.....	19
Figure 2.17 Frequency spectrum of the tie-line flow (Bus 57 to Bus 117) for the case with decoupled damping control.....	19

1.0 Proof of concept

Modern power systems are facing a rapidly growing level of variability and uncertainty due to the increasing level of variable resources and random market forces.

1.1 Background and milestone summary

Low-frequency inter-area oscillations exist in the power grid. Power system stabilizers (PSS) were recognized as a successful real-time modulation control method for the damping of local oscillations, but not for inter-area oscillations. Nowadays, the availability of phasor measurements provides a basis for designing a controller for inter-area oscillations using wide-area signals. However, there has been very little research focusing on the issue that for a large power system with multiple inter-area oscillation modes, a controller designed for one mode may adversely affect other modes.

The objective of this research is to develop decoupled modulation control algorithms for damping inter-area low frequency oscillations, so the damping control can be more effective and easier to design with less interference among different oscillation modes in the system.

The primary technical approach is to separate frequency components and use individual frequency components as inputs for modulation control. The challenges are primarily on how to separate frequency components in real time, how to utilize wide area PMU signals from multiple locations, and how to design a distributed wide-area modulation control algorithm.

Currently, we have developed a signal-decoupling algorithm that has enabled separation of multiple oscillation frequency contents, and extracts a “pure” oscillation frequency mode that is of interest. This decoupled oscillation frequency mode will be fed into the PSS as the modulation input signal. As a result, instead of introducing interferences between different oscillation modes from the traditional approach, the output of the new developed PSS modulation control signal mainly affects only one oscillation mode that we are interested in. The new decoupled modulation damping control algorithm has been tested on the standard IEEE 4-machine 2-area test system with simulated data, and the results have been compared against traditional modulation control on the same test system. The comparison demonstrated the validity and effectiveness of the newly-developed decoupled modulation damping control algorithm. Also we tested the new control algorithms in a minniWECC system. The results show that the proposed algorithm can damp the target mode very well.

1.2 Concept of decoupling oscillation modes

This section briefly describes the concept and method of decoupling different oscillation modes of the system by applying a linear combination of the system state variables.

Power system models can be formulated using the following differential algebraic equations (DAEs):

$$\begin{aligned} \dot{\mathbf{x}} &= \mathbf{f}(\mathbf{x}, \mathbf{y}) \\ \mathbf{0} &= \mathbf{g}(\mathbf{x}, \mathbf{y}) \end{aligned} \tag{1.1}$$

where the vector \mathbf{x} represents state variables describing system dynamics; and the vector \mathbf{y} represents algebraic variables. By linearizing equation (1.1), we have

$$\Delta \dot{\mathbf{x}} = \begin{bmatrix} \frac{\partial f}{\partial \mathbf{x}} & \frac{\partial f}{\partial \mathbf{y}} \end{bmatrix} \begin{bmatrix} \Delta \mathbf{x} \\ \Delta \mathbf{y} \end{bmatrix} \quad (1.2)$$

and

$$\mathbf{0} = \begin{bmatrix} \frac{\partial \mathbf{g}}{\partial \mathbf{x}} & \frac{\partial \mathbf{g}}{\partial \mathbf{y}} \end{bmatrix} \begin{bmatrix} \Delta \mathbf{x} \\ \Delta \mathbf{y} \end{bmatrix} \quad (1.3)$$

From Eq. (1.3), we have

$$\Delta \mathbf{y} = - \left(\frac{\partial \mathbf{g}}{\partial \mathbf{y}} \right)^{-1} \frac{\partial \mathbf{g}}{\partial \mathbf{x}} \Delta \mathbf{x} \quad (1.4)$$

By substituting (1.4) into (1.2), we have

$$\Delta \dot{\mathbf{x}} = \mathbf{A} \Delta \mathbf{x} \quad (1.5)$$

where,

$$\mathbf{A} = \frac{\partial f}{\partial \mathbf{x}} - \frac{\partial f}{\partial \mathbf{y}} \left(\frac{\partial \mathbf{g}}{\partial \mathbf{y}} \right)^{-1} \frac{\partial \mathbf{g}}{\partial \mathbf{x}} \quad (1.6)$$

Time domain solutions of the differential equations shown in Eq. (1.5) have the following closed-form:

$$\begin{aligned} \Delta \mathbf{x}(t) &= u_1 z_1(t) + u_2 z_2(t) + \cdots + u_n z_n(t) \\ &= \mathbf{u} \mathbf{z}(t) \end{aligned} \quad (1.7)$$

where

$$z_i(t) = c_i e^{\lambda_i t} \quad (1.8)$$

c_i determines the initial value of $z_i(t=0)$; λ_i is the i^{th} eigenvalue of matrix \mathbf{A} ; u_i is the right eigenvector of λ_i ; \mathbf{u} is the matrix of right eigenvectors.

We call each $z_i(t) = c_i e^{\lambda_i t}$ as the i -th decoupled mode of the system. And from equation (1.7) and (1.8) we can see that each state variable of the system is a linear combination of all the decoupled modes of the system, and the linear combination coefficients formulate the right eigenvector matrix.

From Eq. (1.7), we have

$$\mathbf{z}(t) = \mathbf{u}^{-1} \Delta \mathbf{x}(t) \quad (1.9)$$

Here $\Delta \mathbf{x}(t)$ represents the system state variables; $\mathbf{z}(t)$ represents the decoupled oscillation. Equation (9) implies that each pure oscillation mode of the system can also be obtained (decoupled) as a linear combination of the system state variables. Assuming the system state variables can be obtained from dynamic state estimation, we can obtain all the decoupled modes of the system. We can choose the dominant decoupled oscillation mode as the feedback input signal in the decoupled modulation control for the PSS.

1.3 An example of a successful proof of concept

For testing the proposed decoupled control algorithm, a two-area, four-machine system was used, shown in Figure 2.1. A PSS is configured at Generator 4 to improve system dynamic performance. The system has mainly three electrical-mechanical oscillation modes (one as the inter-area oscillation mode and the other two as the local oscillation modes).

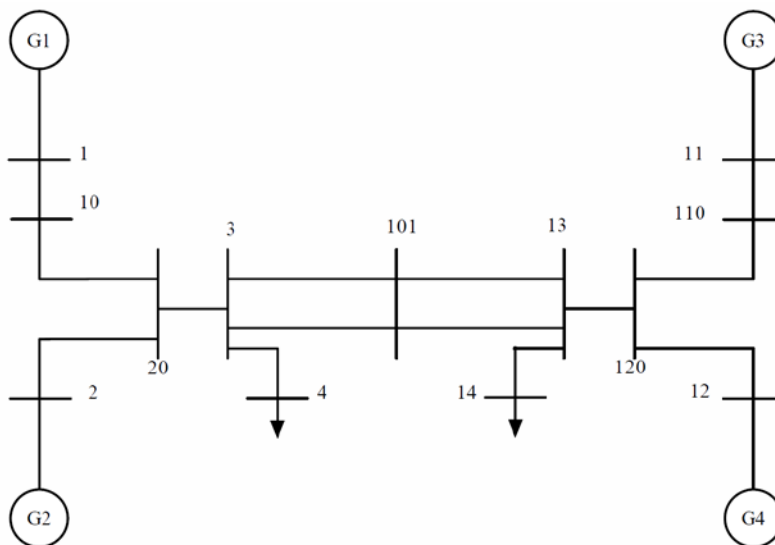


Figure 2.1. Two-area, four-machine system

In the decoupled modulation control method, we apply equation (1.9) to extract the decoupled inter-area oscillation mode and feed it as the input signal for the PSS. As a comparison, we also apply the traditional modulation control method, which feeds the rotor speed of the generator as the feedback signal to the PSS, and as equations (1.7) and (1.8) indicate, the rotor speed (state variable) is actually a combination of all the modes of the system. We implement the small signal stability analysis for both of the above two control methods, and we have the following observations and conclusions:

- (1) The performance of the traditional modulation control is shown in Figure 2.2. As can be seen in Figure 2.2, compared with the base-case system without PSS control, the traditional modulation control for the PSS increases the damping ratio of Mode 1 (inter-area oscillation), but it also has the adverse-effect that making the damping ratio of Mode 2 (local oscillation) decrease, as the eigenvalues of Mode 1 and Mode 2 move in opposite directions in the eigenvalue plane. This is because the inter-area oscillation and local oscillation modes are coupled together in the rotor speed as the feedback signal, and the designed modulation control targeted at damping the inter-area oscillation mode adversely affect the local oscillation mode.
- (2) The performance of the decoupled modulation control is shown in **Figure 2.3**. As can be seen in **Figure 2.3**, compared with the base-case system without PSS control, the decoupled modulation control for the PSS only increases the damping ratio for the target mode 1 (inter-area oscillation), but have no influences for all the other oscillation modes at all, as only the eigenvalue of the target mode moves in the eigenvalue plane. This is as a result of the decoupled modulation control uses only the decoupled “target” mode as the feedback signal.

(3) By comparing the small signal stability analysis results for both the decoupled and traditional modulation controls, we can conclude that the decoupled modulation control method can separate the frequency contents of the system and provide the “pure” target oscillation mode as the input signal to the PSS, and thus effectively eliminate the adverse interferences between different modes of the system.

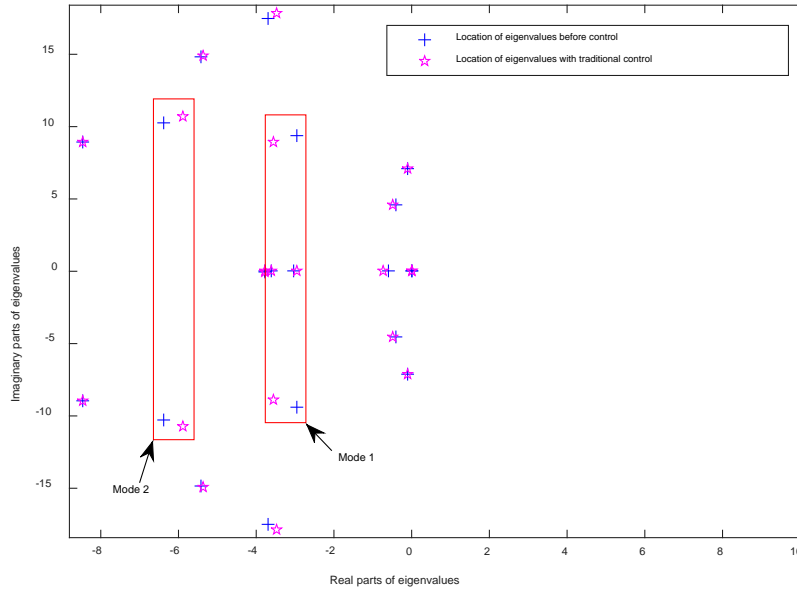


Figure 2.2. Traditional modulation control

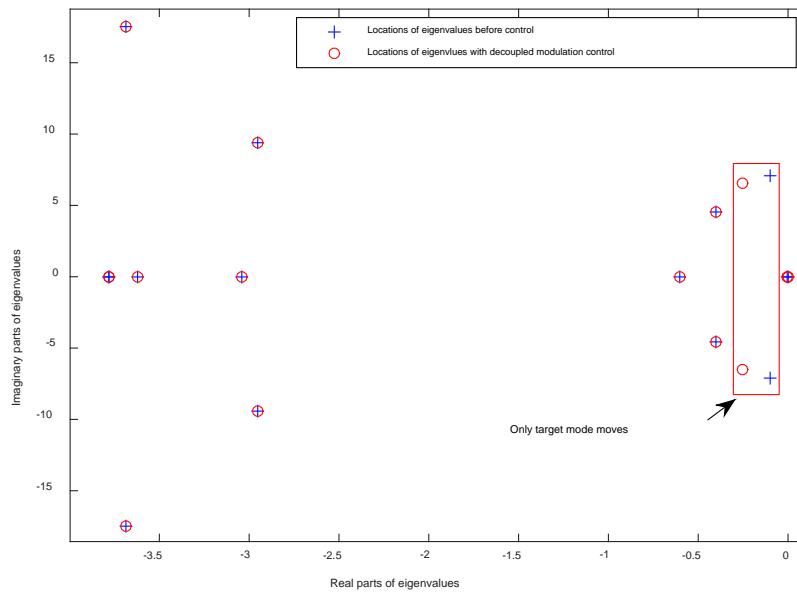


Figure 2.3. Decoupled modulation control

2.0 A real-time signal decoupled approach through band pass filter

This chapter will introduce a band pass filter based decouple approach for decoupled modulation control.

2.1 Real time decoupling approach through band pass filters

The basic idea of this approach is to introduce a band-pass filter before the traditional input signal of PSS. The input signal of the band-pass filter is rotor speed or real power; while the output of the filter is the input for the PSS, which is shown in **Figure 2.1**.



Figure 2.1 Band pass filter

The purpose and functionality of the band-pass filter is to eliminate other frequency components of the input signal while only keep a small range of frequency we are interested in, and thus to provide a “decoupled” signal with a specified narrow range of frequency for the PSS. The transfer function of the filter is shown in

$$F(s) = \frac{\left(\frac{\omega_0}{Q}\right)s}{s^2 + \left(\frac{\omega_0}{Q}\right)s + \omega_0^2}, \quad (1.10)$$

where $f_0 = \omega_0 / 2\pi$ is the center pass frequency; Q is the quality factor. The Bode diagram [1] of this transfer function is shown in **Figure 2.2**. As can be seen from **Figure 2.2**, when the center frequency is fixed, the quality factor determines the pass band. A higher quality factor leads to a narrow pass band and a steeper slope of the frequency. Thus, by filtering and careful selection of the parameters ω_0 and Q , we can get an almost pure modal signal with a designated frequency of f_0 . This pure signal is used as a feedback signal for the PSS input and as a result, the interferences between different oscillation modes (frequencies) are dramatically reduced.

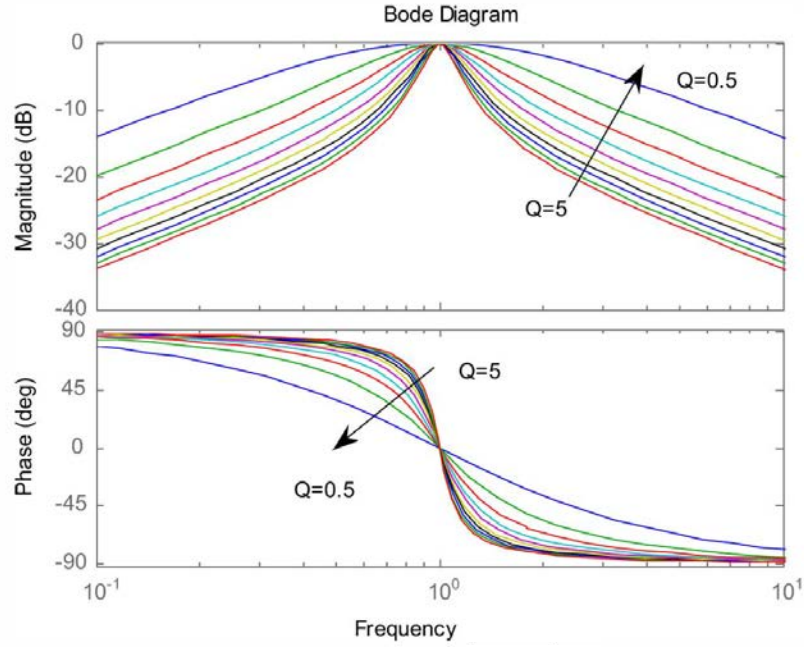


Figure 2.2 Frequency characteristic with $\omega_0=1$ and various values of Q , for 0.5 to 5. [1]

2.2 Implementation of the approach

The transfer function shown in (1.10) can be translated into state-space model shown in the following:

$$\begin{cases} \dot{x} = Ax + Bu \\ y = Cx \end{cases}, \quad (1.11)$$

where

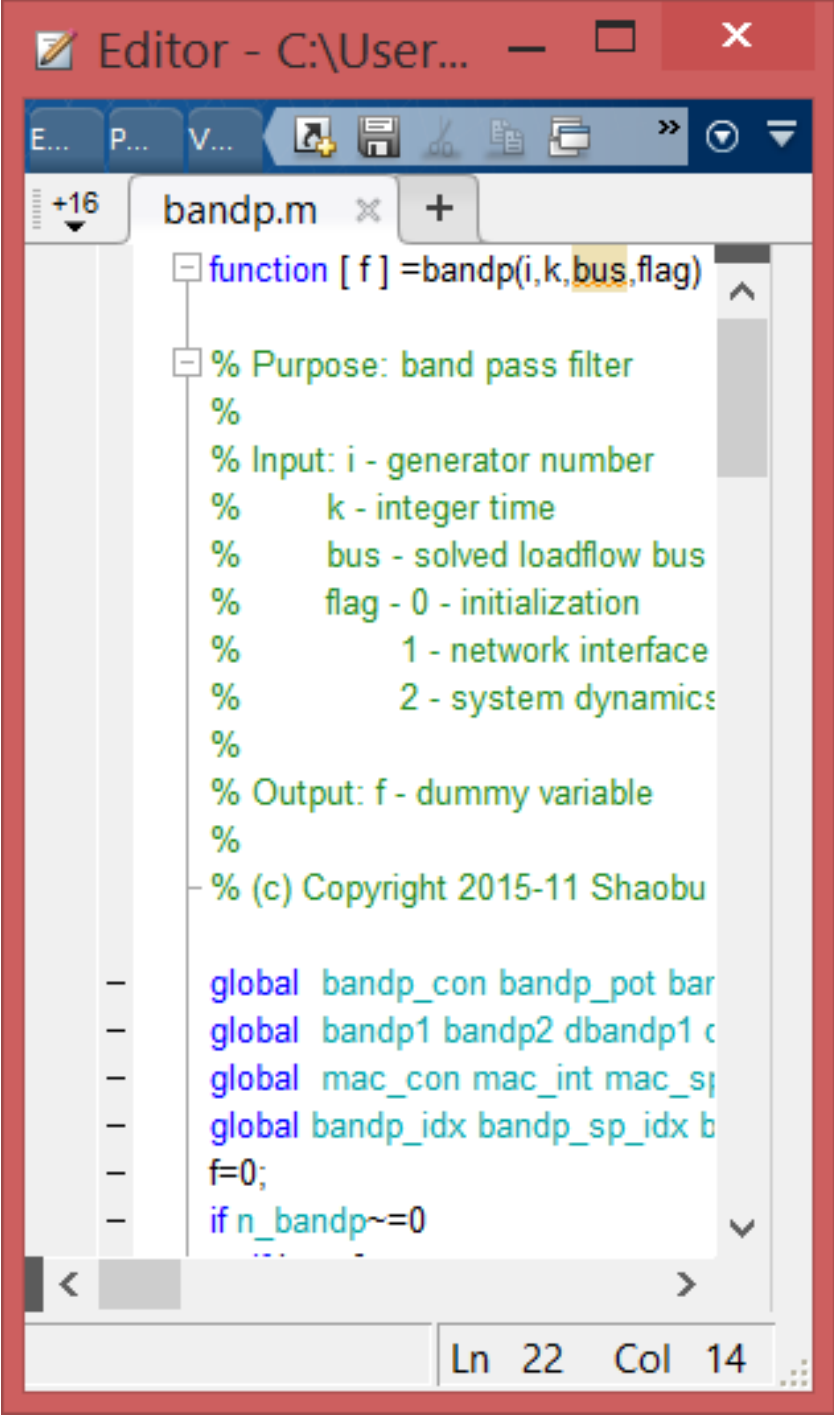
$$x = \begin{bmatrix} \dot{x}_1 \\ \dot{x}_2 \end{bmatrix} \quad (1.12)$$

$$A = \begin{bmatrix} -\left(\frac{\omega_0}{Q}\right) & -\omega_0^2 \\ 1 & 0 \end{bmatrix} \quad (1.13)$$

$$B = \begin{bmatrix} 1 \\ 0 \end{bmatrix} \quad (1.14)$$

$$C = \begin{bmatrix} \frac{\omega_0}{Q} & 0 \end{bmatrix} \quad (1.15)$$

By adding an M file shown in **Figure 2.3** to the power system toolbox (PST), which is designed for power system dynamic simulation, the dynamic equations (1.11)-(1.15) of the band-pass filter can be integrated into PST and the dynamic behavior of the closed-loop control system with the band-pass filter can be simulated.



```
function [ f ] =bandp(i,k,bus,flag)
% Purpose: band pass filter
%
% Input: i - generator number
%        k - integer time
%        bus - solved loadflow bus
%        flag - 0 - initialization
%              1 - network interface
%              2 - system dynamics
%
% Output: f - dummy variable
%
% (c) Copyright 2015-11 Shaobu

global bandp_con bandp_pot bandp_sp_idx
global bandp1 bandp2 dbandp1 cbandp1
global mac_con mac_int mac_sp_idx
global bandp_idx bandp_sp_idx bbandp1
f=0;
if n_bandp~=0
```

Figure 2.3 M file for the band pass filter

2.3 Test results in the two-area four-machine system

The above band-pass-filter-based approach is tested with a two-area-four-machine system [1], which is shown in the following figure. The proposed the band-pass filter and PSS, which are specially designed for each oscillation mode separately, are added to the system, with each test case only focusing on one mode, and the oscillations of the tie-line power flow are analyzed. It is clearly shown from the results that the band-pass filter and PSS designed for a designated frequency mode of interest can efficiently suppress the oscillations of that mode, while they bring no interferences for other oscillation modes.

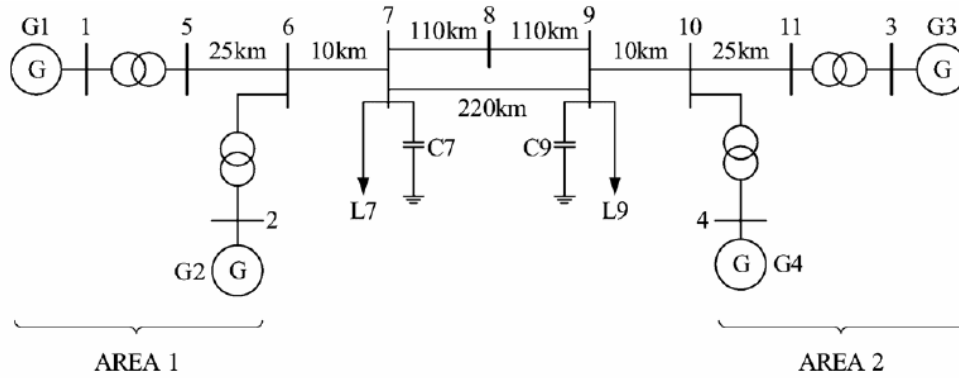


Figure 2.4 Two-area four-machine system

Without the PSS and band-pass filter, the oscillation of the tie-line power following a small disturbance is shown in **Figure 2.5**. The frequency spectrum of the oscillation is shown in **Figure 2.6**. It is clearly shown in **Figure 2.6** that there are two modes of oscillation: one is 0.72 Hz, and the other one is 1.15 Hz.

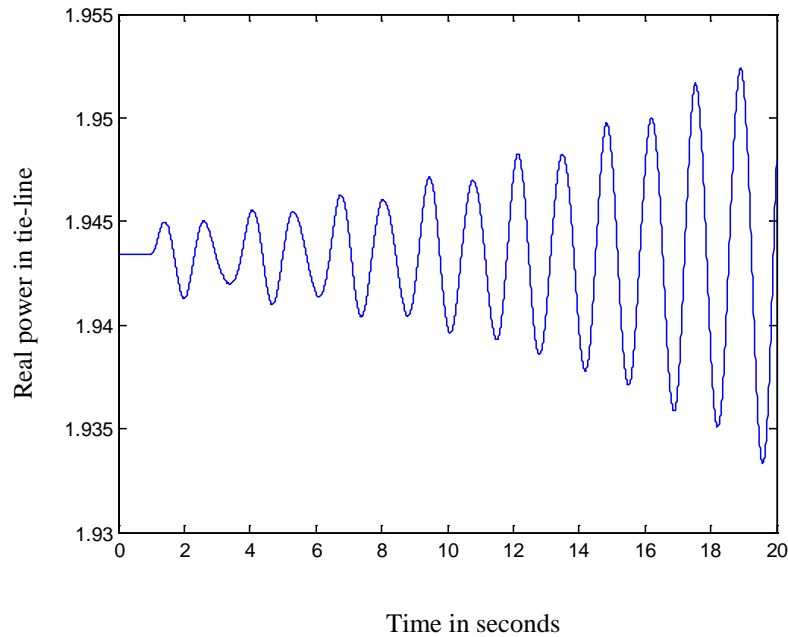


Figure 2.5 Tie-line power oscillation without PSS

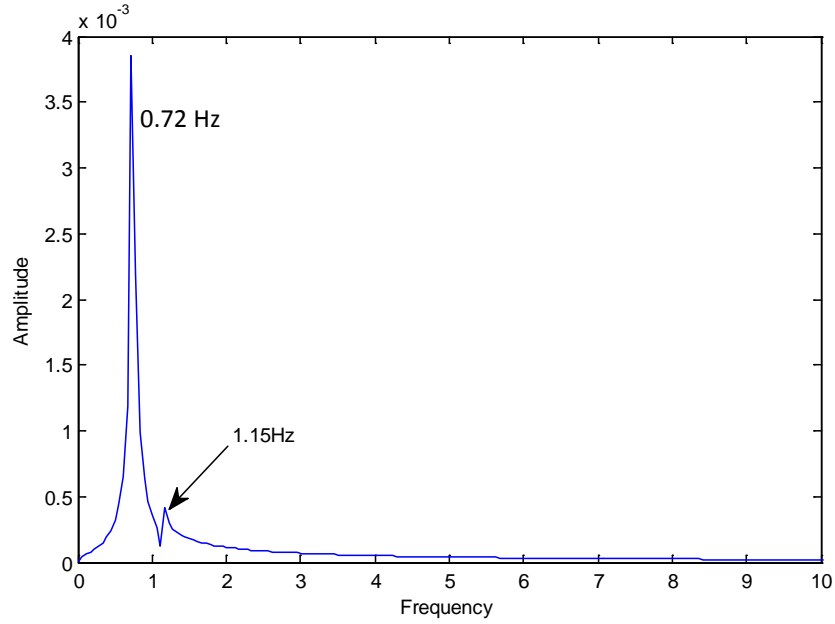


Figure 2.6 Frequency spectrum of the tie-line power oscillation in Fig. 2.5

The band-pass filter and the PSS designed for a specified frequency (0.72 Hz or 1.15 Hz) are added into the system to test whether the proposed method can suppress these two modes discriminately. The band-pass filter and the PSS are first designed to aim at suppressing the oscillation with 1.15 Hz frequency as the target mode. A PSS with a band-pass filter is configured on Generator 1. For the band-pass filter, we set

$$\omega_0 = f \times 2\pi = 1.15 \times 2\pi = 7.23. \quad (1.16)$$

Following the same disturbance, the tie-line power oscillation is shown **Figure 2.7**. The frequency spectrum of the oscillation is shown in **Figure 2.8**. As can be seen from **Figure 2.8**, the mode with frequency of 1.15 Hz has been removed, while the one with 0.72 Hz is not affected.

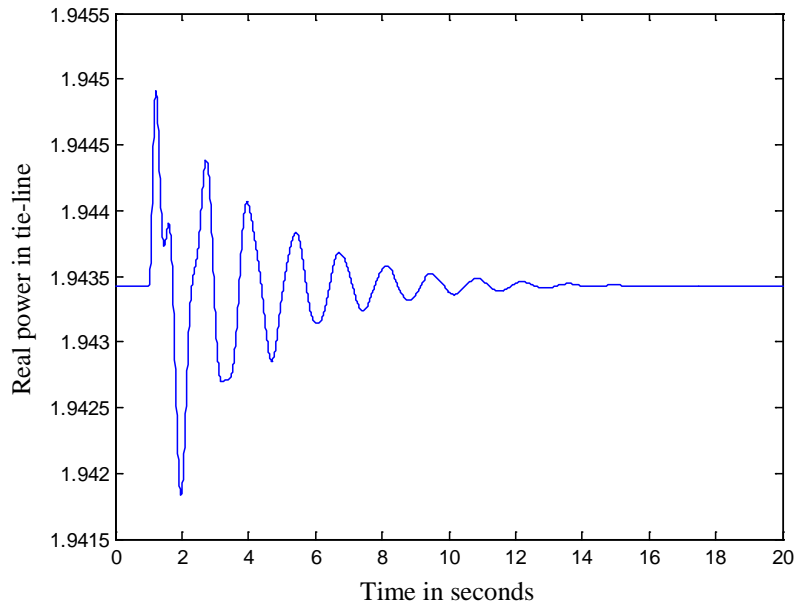


Figure 2.7 Tie-line power oscillation with band-pass filter of 1.15 Hz

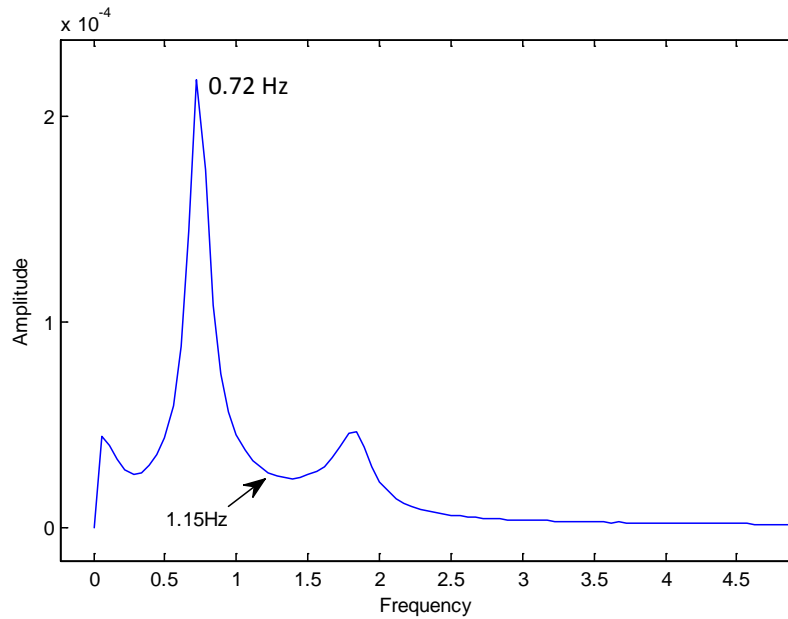


Figure 2.8 Frequency spectrum of the tie-line power oscillation in Fig. 2.7

In the next step, the band-pass filter and the PSS are designed to aim at suppressing the oscillation with 0.72 Hz frequency as the target mode. As the 0.72 Hz is an inter-area oscillation mode, each generator is configured with a PSS and a band-pass filter. For each band-pass filter, we set

$$\omega_0 = f \times 2\pi = 0.72 \times 2\pi = 4.52 . \quad (1.17)$$

Following the same disturbance, the tie-line power oscillation is shown in **Figure 2.9**. The frequency spectrum of the oscillation is shown in **Figure 2.10**. As can be seen from **Figure 2.10**, the mode with frequency of 0.72 Hz has been removed, while the frequency of 1.15 Hz is not affected.

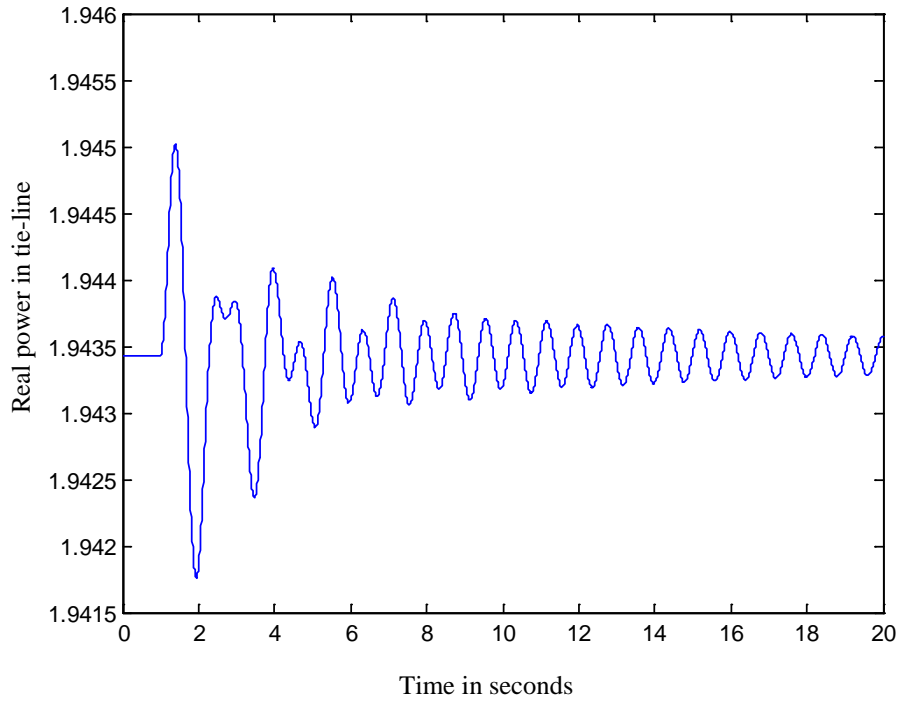


Figure 2.9 Tie line power oscillation with four PSSs

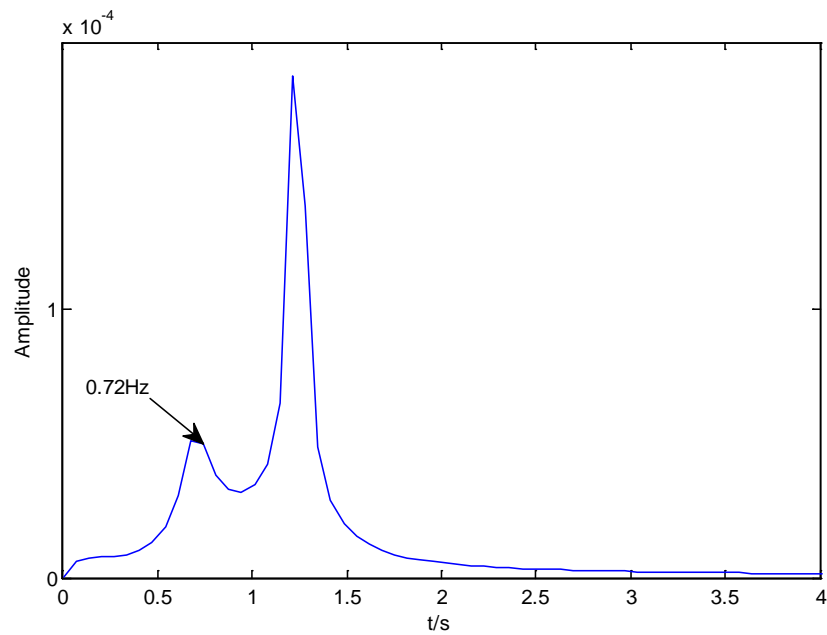


Figure 2.10 Frequency spectrum of the power oscillation in Fig. 2.9

Figure 2.11 shows the performance comparison between decoupled control (with band-pass filter) and PSS designed for only the inter-area oscillation mode, 0.72 Hz) and the traditional modulation control. As can be seen from **Figure 2.11**, the decoupled control approach can provide a better damping ratio, as the decouple modulation can eliminate the interferences from the other 1.15 Hz oscillation mode.

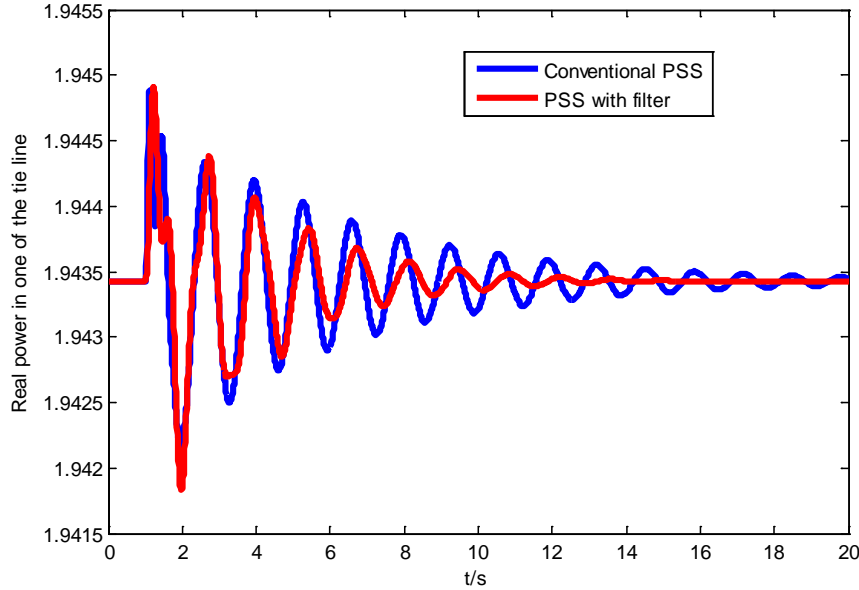


Figure 2.11 Performance comparison

2.4 Test results in the minniWECC system

A mid-size simplified minniWECC system [2], shown in Figure 2.12, is used to further evaluate the performance and the scalability of the proposed algorithm. It is verified from the simulation results of the minniWECC system with decoupled damping control that the decoupled damping control could mainly affect only one oscillation mode that we are interested in, without introducing interferences between different oscillation modes.

Table 2.1. Summary of voltage violation frequency for 500 kV level buses

Mode	Frequency (Hz)	Damping (%)
N-S	0.170	24.0
Alberta	0.324	0.5
E-W south 1	0.501	7.5
Montana	0.549	7.0
BC	0.626	2.0
E-W south 2	0.683	5.0
Middle	0.709	4.0

The system consists of 34 generators, 120 buses, 115 lines and transformers, 54 generator and load transformers, 19 load buses, and 2 DC lines. Two types of generator models (i.e., salient pole model and

round rotor model) are used. Each generator is equipped with an exciter model. Three generators are equipped with power system stabilizers (PSS) to damp local oscillation modes.

Table 2.1 shows all the seven inter-area oscillation modes for the minniWECC system. Among all the seven oscillation modes, it is observed from

Table 2.1 that the “Alberta” and “BC” modes have the lowest damping ratios, 0.5% and 2.0% respectively. **Figure 2.13** and **Figure 2.14** show the mode shapes of the “Alberta” and “BC” modes, respectively.

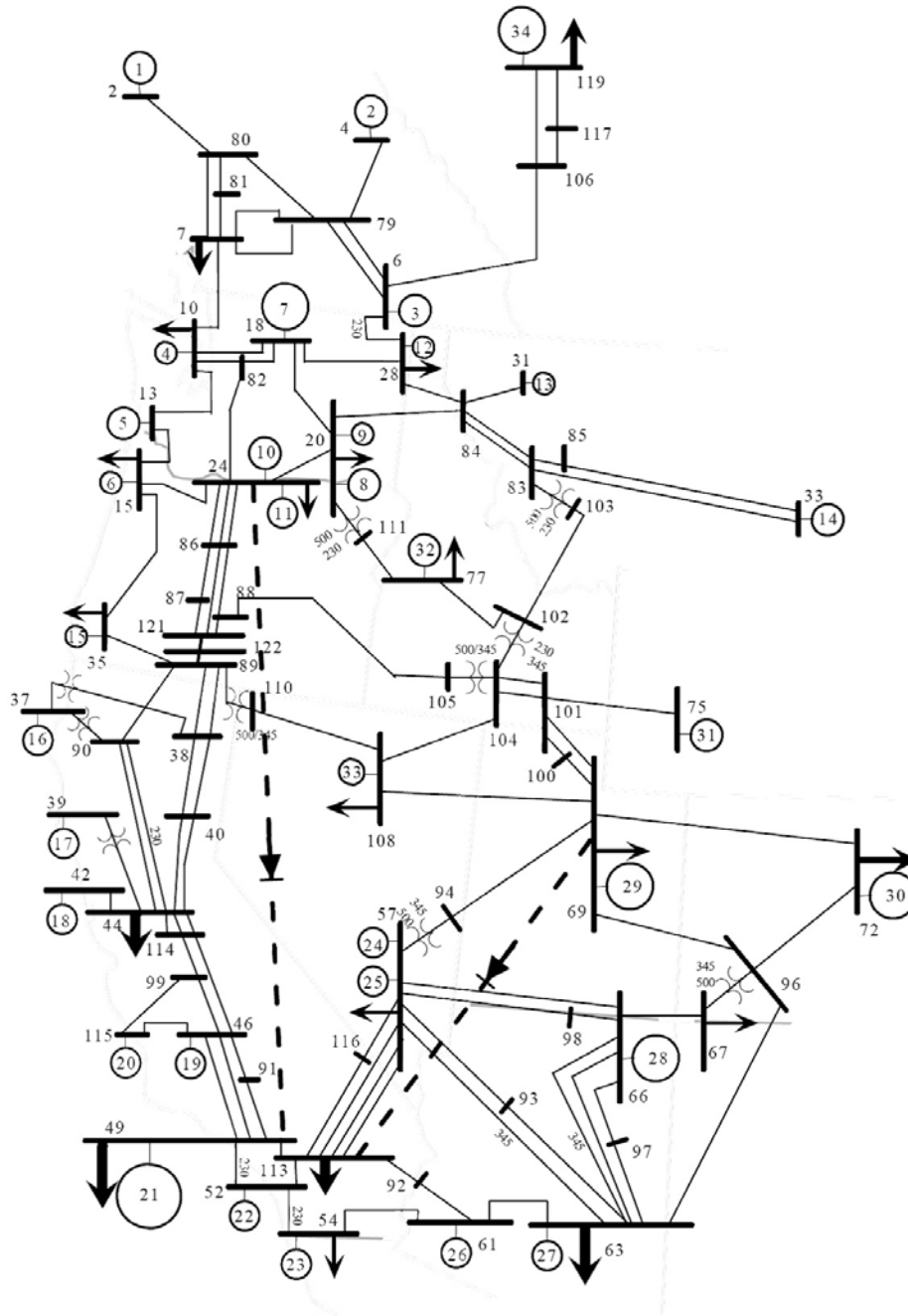


Figure 2.12 Simplified WECC System One-Line Diagram [2]

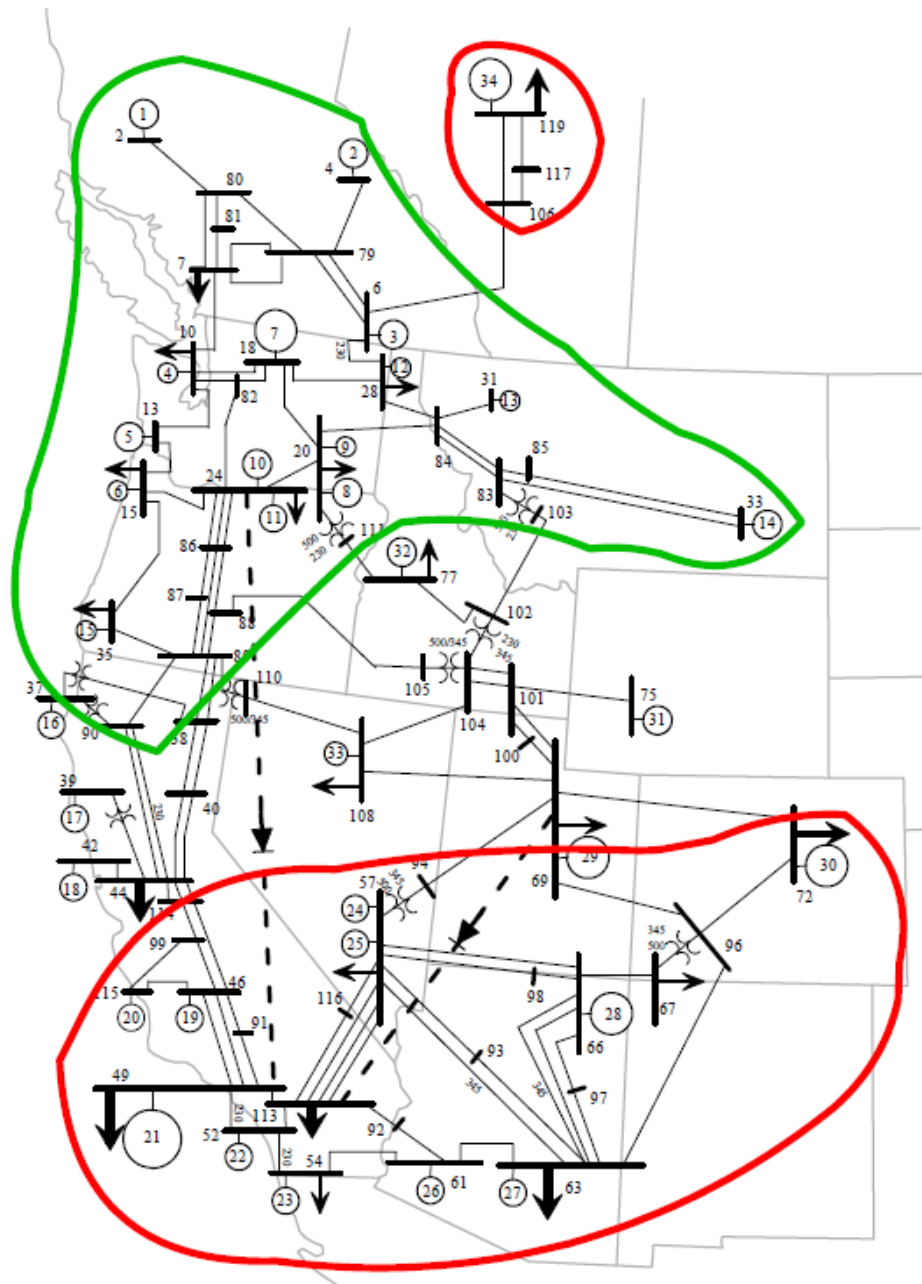


Figure 2.13 Mode shape for 0.324-Hz Alberta mode in minniWECC system

simulation results are compared as follows. It is verified from the simulation results of the minniWECC system with decoupled damping control that the decoupled damping control could mainly affect only one oscillation mode that we are interested in, without introducing interferences between different oscillation modes.

Figure 2.15 shows the power flows of one of the three tie-lines from LV (Bus 57) to LA (Bus 113), for both the case without PSS and the case with band-pass filter and PSS. It is clearly shown from Figure 2.15 that for the case without PSS and decoupled damping control, there exist two oscillation modes with different frequencies, while for the case with band-pass filter and PSS (decoupled damping control), after about 15 seconds of oscillation, one frequency oscillation mode disappears on the tie-line power flow.

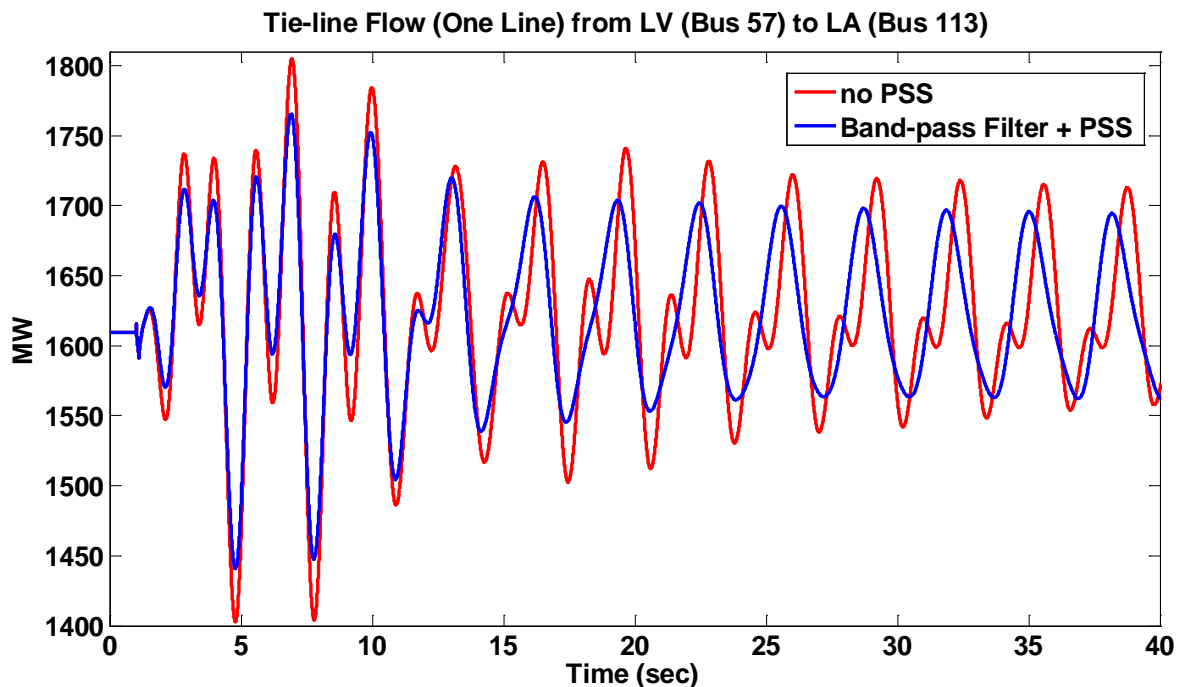


Figure 2.15 Tie-line flow (one line) from LV (Bus 57) to LA (Bus 113).

Further investigations are conducted for the tie-line power flow for both cases: frequency spectrum analysis is implemented for the tie-line flow and the results are shown in Figure 2.16 and Figure 2.17. From Figure 2.16 it is clearly shown that for the case where the minniWECC system does not have a decoupled damping control for the specified 0.6-Hz BC mode, there exists two poorly-damped low-frequency oscillation modes in the system: 0.32-Hz Alberta mode and the 0.64-Hz BC mode, as the frequency spectrum of the tie-line flow has two main components: 0.32 Hz and 0.64 Hz. The amplitude ratio of the 0.64 Hz to 0.32 Hz is about $0.3246/0.517 = 0.6279$. Figure 2.17 shows how the decoupled damping control helps to damp the 0.64-Hz BC target mode of oscillation but not has impact on the other modes: the amplitude of the 0.64-Hz component in the spectrum of the tie-line power flow with decoupled damping control is highly depressed, while the amplitude of the 0.32-Hz component keeps almost the same. The amplitude ratio of the 0.64 Hz to 0.32 Hz in this case is now only $0.09783/0.6033 = 0.1622$, which is 3.87 times smaller than the case without the decoupled damping control. Note that the difference of the amplitude of 0.32 Hz in the two cases is due to the normalization of the energy of the different frequency components in the spectrum analysis, as the 0.32-Hz oscillation becomes the

dominant mode for the case with decoupled damping control. It does not mean the 0.32-Hz oscillation is enhanced by the decoupled damping control, and this is verified by Figure 2.15: the amplitude of the tie-line power flow in the case with decoupled damping control never exceeds the amplitude of the tie-line power flow in the case without decoupled damping control.

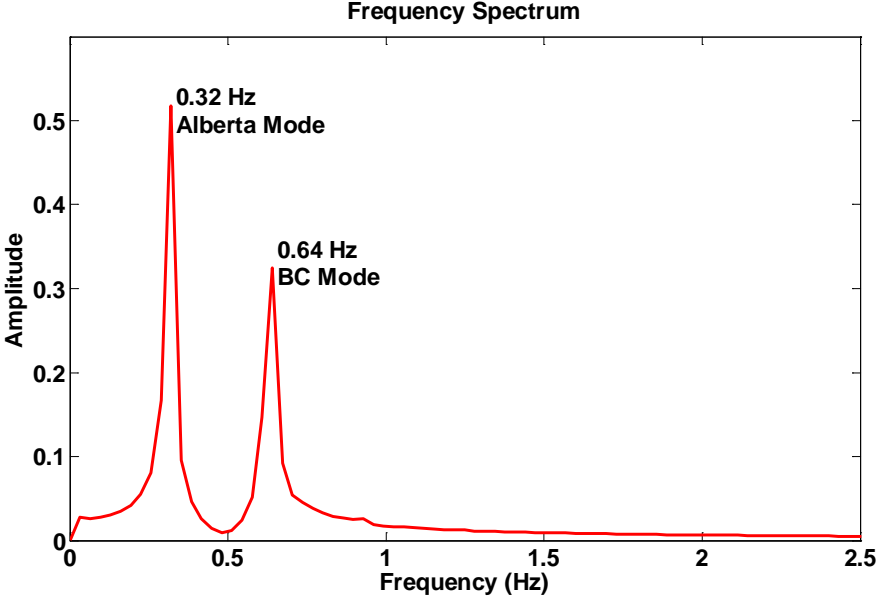


Figure 2.16 Frequency spectrum of the tie-line flow (Bus 57 to Bus 117) for the case without decoupled damping control

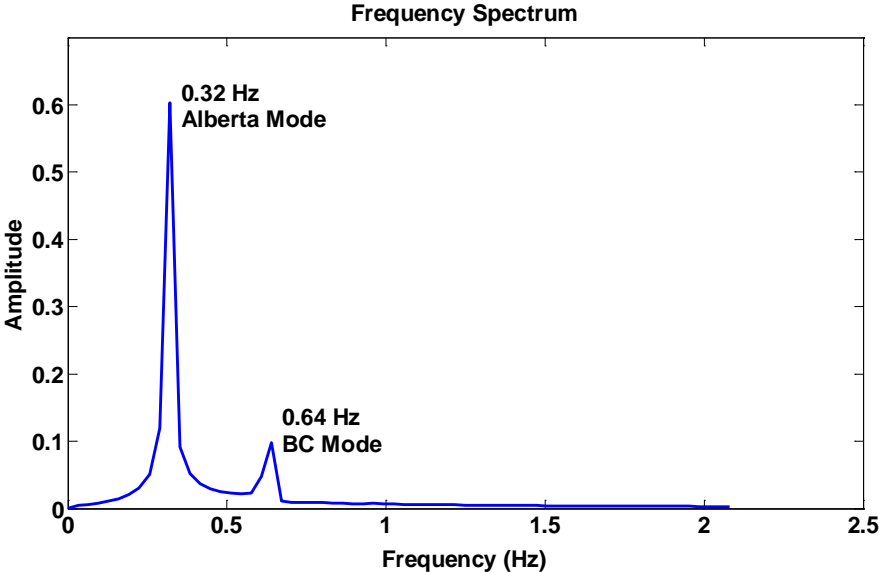


Figure 2.17 Frequency spectrum of the tie-line flow (Bus 57 to Bus 117) for the case with decoupled damping control

3.0 Conclusions

In this project, we developed a decoupled modulation control method. First, through the proof of concept study we demonstrated how the pure mode signals improve system performance. Then we developed a real-time signal decoupling control method, and tested the method on a two-area four-machine system and a minniWECC system. By comparing the proposed approach with traditional modulation control, we can reach the following conclusions.

- (1) In traditional modulation control, modes are coupled together. Sometimes, feedback signals increase the damping ratio of one mode, but decrease the damping ratio of others. This is because the inter-area oscillation and local oscillation modes are coupled together in the feedback signals, and the traditional modulation control cannot handle them discriminately.
- (2) In the proposed decoupled control, modes are handled separately so that one feedback signal is able to increase the damping ratio for the target mode 1, without influences on all the other oscillation modes. This is because the feedback signal only contains the pure target mode, instead of a combination of all the modes as the feedback signals.
- (3) Through eliminating the adverse interferences between different modes of the system, the decoupled modulation control is able to provide better control performance.

4.0 References

- [1] J. Zhang, C. Y. Chung and Y. Han, “A Novel Modal Decomposition Control and Its Application to PSS Design for Damping Inter-area Oscillations in Power Systems,” *IEEE Trans. Power Syst.*, vol. 27, no. 4, pp. 2015–2025, 2012.
- [2] Trudnowski, D.J. and J. Undrill, *The minniWECC System Model*, technical report, September 2008.



Pacific Northwest
NATIONAL LABORATORY

*Proudly Operated by **Battelle** Since 1965*

902 Battelle Boulevard
P.O. Box 999
Richland, WA 99352
1-888-375-PNNL (7665)

www.pnl.gov



U.S. DEPARTMENT OF
ENERGY